

Nanoscale patterning and deformation of soft matter by scanning probe microscopy

S. Kassavetis ^{*}, K. Mitsakakis, S. Logothetidis

Aristotle University of Thessaloniki, Department of Physics, Laboratory for Thin Films – Nanosystems and Nanometrology, GR-54124, Thessaloniki, Greece

Received 13 May 2006; received in revised form 1 August 2006; accepted 1 August 2006
Available online 27 September 2006

Abstract

In this work, atomic force microscopy (AFM) was used for the surface nanopatterning as well as to study the nanoscale deformation of soft, carbon-based thin films and polymeric (polyethylene terephthalate, PET) membranes. The process of the AFM nanolithography was realized by application of contact force pulses to the samples, using silicon rectangular cantilevers of relatively high spring constant ($k_c = 11$ N/m, nominal value).

Simultaneously, AFM is functioned as a nanometrology instrument, for nanomechanical measurements of the applied force and pressure for plastic deformation of the surface, which were found to vary between 200 and 2500 nN and between 1 and 4 GPa, respectively. The derived data were cross-checked with the materials' nanomechanical properties, which were measured using depth-sensing Nanoindentation, and the limits of the possible applied forces were specified.

During the herein presented AFM nanolithography, several types of well-defined shapes, like pits and lines, were made. The dimensions of the patterned structures were correlated with the nanolithography parameters (e.g. applied force). The contact mechanics for the formation of uniformly patterned surfaces are discussed, in terms of shape geometry and dimensions, which comprise the essential characteristics for advanced applications like “probe-based data storage”, where data storage capacity is determined by pattern dimensions, or preferential adsorption of biomolecules on a patterned surface.

© 2006 Elsevier B.V. All rights reserved.

Keywords: SPM; Nanoindentation; Force lithography; Pile-up; Amorphous carbon; Polymer

1. Introduction

Scanning probe microscopy (SPM) [1,2] has been used in a wide variety of applications for materials characterization. With the proper modifications or configurations, SPM can be used, apart from surface imaging, for characterization of local surface magnetic, electric and mechanical properties as well. During the last decade, SPM applications have been further expanded to surface design by means of SPM lithography, a very promising technique for applications in the field of micro/nanoelectronics for patterning very discreet features [3–5], for polymer surface “writing” [6,7] and in biocompatible materials, where surface periodical patterns may or not promote adsorption of biological molecules [8].

In this study, SPM nanolithography was performed on flexible polyethylene terephthalate (PET) membranes (12 μm thick), which are already used as substrates for the production of flexible electronic devices, and on rigid materials – soft amorphous hydrogenated carbon (a-C:H) thin films grown on crystalline Si(001) substrates. All the surface-modified materials were reported in the bibliography that exhibits biocompatible properties [9]. From the SPM lithography parameters, the

Table 1
Deposition parameters of the a-C:H samples and the equivalent hardness values

Samples	Bias voltage (V)	Hardness (GPa)
#1 a-C:H	–40	4.4
#2 a-C:H	–20	3.0
#3 a-C:H	$V_b > 0$	1.8
PET 12 μm	–	0.4

^{*} Corresponding author. Tel.: +30 2310 998239; fax: +30 2310 998390.
E-mail address: skasa@physics.auth.gr (S. Kassavetis).

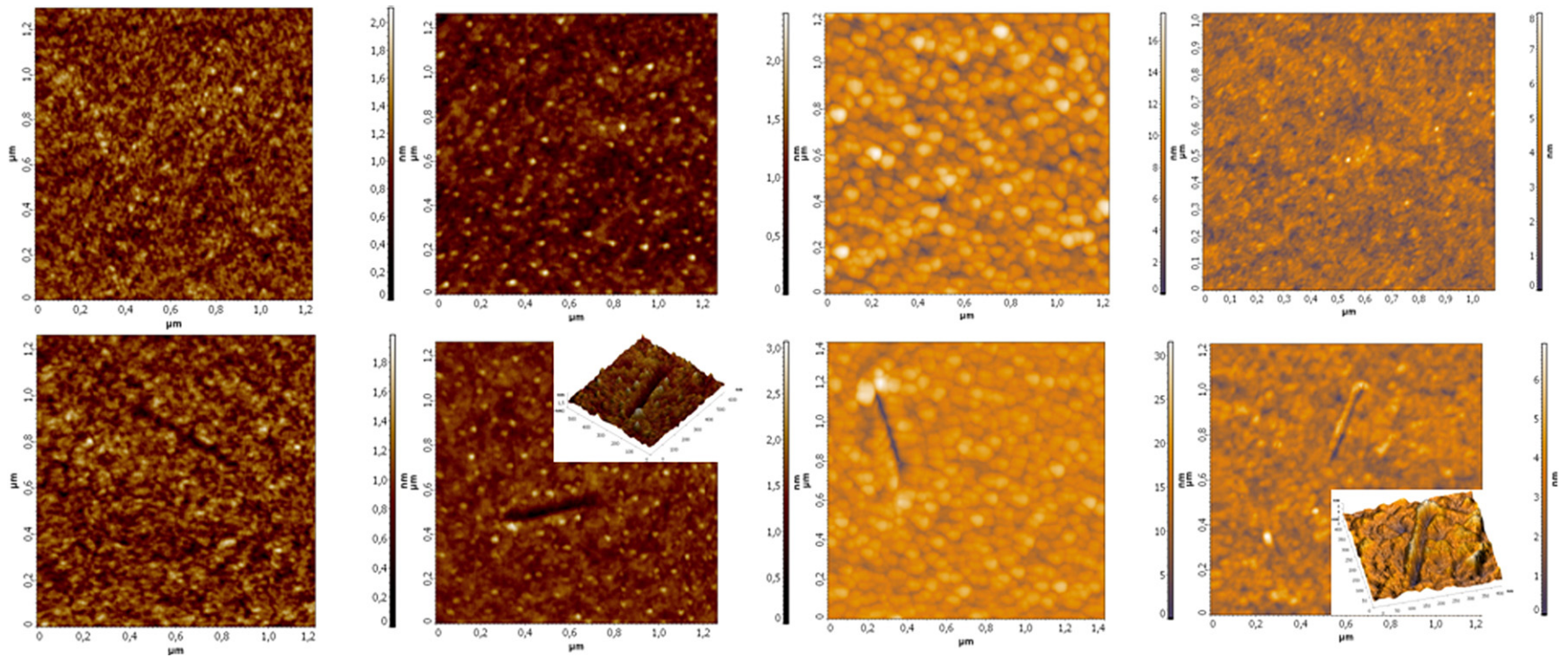


Fig. 1. $1 \times 1 \mu\text{m}^2$ 2D topography images of the samples before (upper row) and after (lower row) SPM nanolithography. The columns refer to samples #1, #2, #3 a-C:H and PET from left to right, respectively.

applied force, F_a , and pressure, P_a , were calculated by using the appropriate assumptions and equations. Afterwards F_a and P_a were correlated with the morphology features of the patterns and the hardness (H) of the tested materials, which was derived using depth-sensing Nanoindentation. The combination of results from SPM and Nanoindentation, as the two nanomechanical property characterization techniques, is evaluated [10].

Finally, in the case of the PET membrane a series of pits was made by varying the applied force. The geometrical characteristics of the pits and the formation of the pile-up regions were discussed, in terms of the applied force.

2. Experimental

The growth of a-C:H thin films on Si(001) substrates took place in a high vacuum chamber ($P < 2 \times 10^{-7}$ mbar) by means of RF reactive magnetron sputtering of 99.999% pure graphite target. Argon was used as the inert gas and H_2 as reactive one. The a-C:H thin films were grown with or without negative bias voltage (V_b) at the substrate. The tested PET samples were commercially available semicrystalline, biaxially oriented, $\sim 12 \mu\text{m}$ thick membranes. The hardness of the samples was evaluated with depth-sensing Nanoindentation test, using a Berkovich-type diamond tip and the “Continuous Stiffness Measurements” option of the Nano Indenter Xp apparatus [11,12]. In order to avoid any bending of the PET membrane during indentation, the samples were glued to the sample holders [13].

The surface imaging and patterning procedures were realized with the scanning-by-probe system SOLVER P47H SPM from NT-MDT. Both Contact and Semi-Contact mode were utilized. More specifically, the initial scanning to detect a smooth enough surface for the nanolithography procedure was carried out in Semi-Contact mode. Then, the lithography parameters were established (e.g. the shape of the pattern to be engraved, the applied force, etc.) and the mode was switched automatically to scan in Contact mode, in order to perform the patterning, in the form of “vector” lithography (i.e. force pulses of equal magnitude and duration). The lithography results were “visualized” again by scanning in Semi-Contact mode. The basic difference

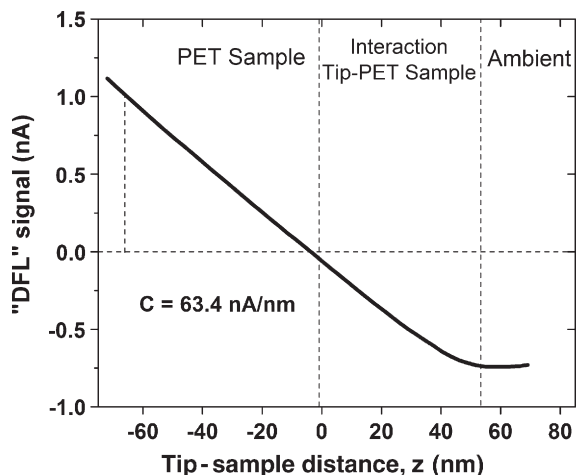


Fig. 2. “DFL” signal (force) – distance curve for the case of the PET sample.

Table 2

Applied force and pressure by the AFM tip on each sample

Samples	Applied force, F_a (nN)	Pressure, P_a (GPa)
# 1 a-C:H	2520±702	4.0±1.0
# 2 a-C:H	1551±442	2.5±0.7
# 3 a-C:H	1094±306	1.7±0.5
PET 12 μm	760±255	1.2±0.4

between these two operating modes is that during Semi-Contact the tip is oscillating above the sample and taps it once in every oscillation circle, thus, reducing the danger of sample destruction, especially in the case of the PET membranes. On the other hand, in Contact mode scanning, the tip is in constant contact with the surface, enhancing the possibility of scratching.

Force lithography was performed using Si rectangular cantilevers, with relatively high spring constant ($k_c = 11 \text{ N/m}$) nominal value and nominal resonance frequency f_o of 226 kHz. The latter is directly and accurately measured by the software itself enabling a more precise estimation of the k_c value than the nominal one.

3. Results and discussion

In Table 1 the hardness, measured by Nanoindentation tests, and the V_b during the growth of the a-C:H samples are presented. The effect of the V_b to the nanomechanical properties of the a-C:H thin films has been discussed elsewhere [12].

The AFM images of the samples before and after the nanopatterning appear in Fig. 1, where the first row depicts the surface image of each sample before, and the second column the same the surface region after nanolithography.

One of the most important parameters for AFM nanolithography is the applied by the tip force to the sample. Therefore, the nanolithography process took place in such a way that the created scratches had the same depth and width (1 nm and 40 nm, respectively), so as to estimate the F_a with respect to the ascending H values of the four different samples.

Firstly the proportionality of the current signal “DFL” to the cantilever deflection was derived by the DFL (nA) – distance (nm) curve, also named Force – distance ($F-d$) curve. A representative $F-d$ curve is presented in Fig. 2. The horizontal line in Fig. 2 refers to the condition of “tip far from sample” (ambient), when no interaction between the tip and the sample exists (no change in “DFL” signal). The sloped line represents the increase of cantilever deflection (and therefore of F_a), while being in contact and penetrating to the sample. Then, the F_a was calculated according to Hooke’s law, regarding the cantilever as an elastic spring, and in this way the “DFL” signal is transformed into force values (Eq. (1)). The $F-d$ curves for all samples have the same form as that in Fig. 2 and all the above are summarized in the following formula;

$$F_a \text{ (nN)} = k_c \text{ (N/m)} \cdot C \text{ (nm/nA)} \cdot \text{DFL (nA)} \quad (1)$$

where “DFL” is set by the user according to the desired level of force to be applied.

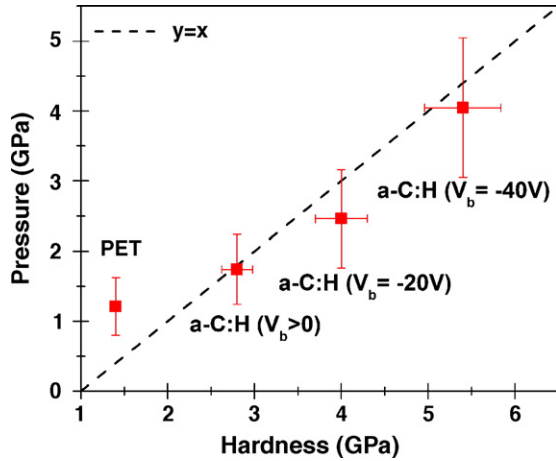


Fig. 3. Pressure applied on a-C:H and PET samples by the AFM tip vs. the hardness of materials measured by nanoindentation.

From (1) it comes out that it is necessary to define precisely the value of k_c . For this purpose the following equation was used;

$$k_c = m^* \omega_0^2 = m^* \cdot 4\pi^2 f_0^2 = \frac{m}{4} \cdot 4\pi^2 f_0^2 = \rho \cdot l \cdot w \cdot t \cdot \pi^2 f_0^2 \quad (2)$$

where ρ is the cantilever material’s mass density, l , w and t are the length, width and thickness of the cantilever, f_0 is its resonance frequency and m^* is the “effective mass” of the cantilever–tip system equal to $m/4$ [14]. Density is taken to be 2330 kg/m^3 [15] and cantilever dimensions nominal values (including error values) are; $l \pm \Delta l = (100.0 \pm 5.0) \mu\text{m}$, $w \pm \Delta w = (35.0 \pm 3.0) \mu\text{m}$, $t \pm \Delta t = (2.0 \pm 0.3) \mu\text{m}$. Thus, from Eq. (2), $k_c = 8.2 \pm 2.3 \text{ N/m}$. The error in k_c propagates to the calculation of the F_a values, presented in Table 2.

In practice, “nanolithography” means permanent nanoscale plastic deformation of the material surface. Such a drastic change in the surface conformation is achieved only if the exerted pressure P_a by the tip exceeds a certain limit, typical of each sample; its hardness. In order to proceed to the estimation of P_a , the following assumptions were made: the shape of the AFM tip edge is regarded as hemispherical, the tip radius R is

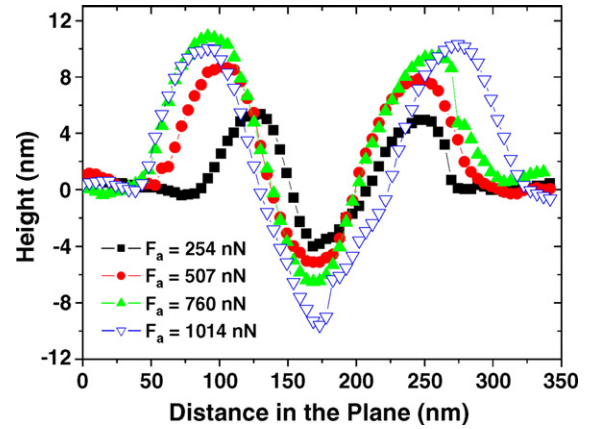


Fig. 5. Profiles of the surface pits on PET vs. normalized distance in the plane (upper scale corresponds to pit made by $F_a = 1041 \text{ nN}$).

considered 10 nm , equal to the nominal value, and the contact area S is also assumed to be hemispherical, equal to $S = 2\pi \cdot R_{\text{tip}}^2$. Thus the P_a is calculated using Eq. (3):

$$P_a \text{ (GPa)} = \frac{\text{Applied Force}}{\text{Contact Area}} = \frac{F_a}{2\pi \cdot R_{\text{tip}}^2} \quad (3)$$

The P_a values are presented in Table 2.

In Fig. 3, results related to the permanent plastic deformation of the soft materials surface by the SPM Si rectangular cantilever and the diamond Berkovich-type Nanoindenter tip are presented and can be cross-checked. The line $y=x$ stands for P_a values equal to H . According to the previously mentioned condition ($P_a \geq H$) for permanent surface deformation, the P_a values should lie either on, or above this line. Indeed, this is the case within the error limits, showing that the results from SPM are in accordance with those from the Nanoindenter. Moreover, for the reasonable question “how such low forces, of the order of a few hundreds of nN, can deform permanently the surface of hard materials with hardness ranging from 1 to 4 GPa?”, the answer lies in the nanoscale contact area between the tip and the surface.

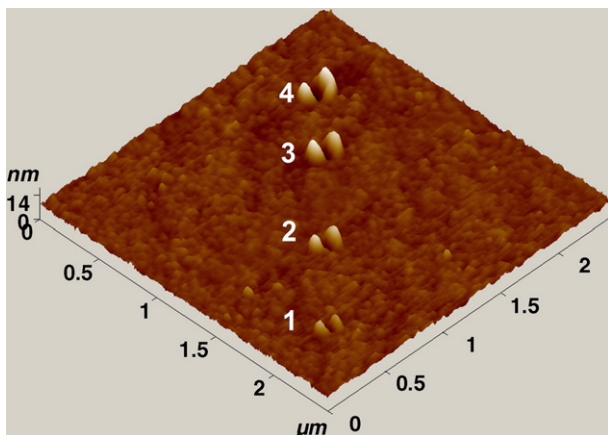


Fig. 4. 3D AFM topography image of an array of four surface pits on the PET sample.

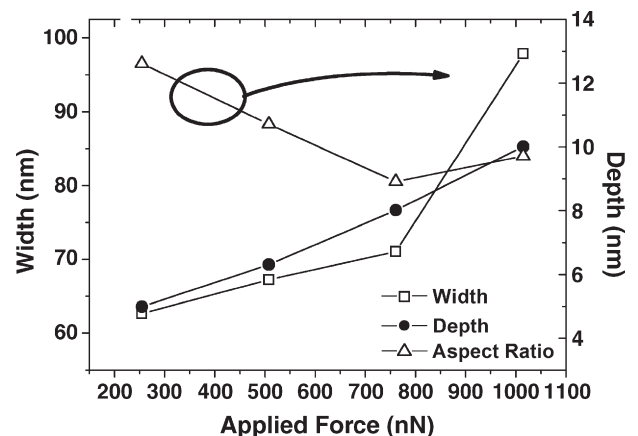


Fig. 6. The width, the depth and the aspect ratio of the indented surface pits (shown in Fig. 4) with respect to the applied force, F_a .

Further efforts for SPM nanolithography on samples with $H > 5$ GPa using the same cantilever were made but to no point. An upper limit of the applied force and pressure is set, firstly, by the SPM apparatus itself (and in particular, by the maximum detectable cantilever deflection symbolized by “DFL”) and for this cantilever was around 5000 nN (with maximum exerted pressure $P_{\max} = 7.9$ GPa). On the other hand, limitation to the maximum P_a comes from the cantilever itself and specifically from its spring constant; higher k_c means that the same force can be achieved with less cantilever deflection.

In order to study further the effect of the applied force to the geometrical characteristics of the patterns, a series of 4 pits/indents with varying F_a was made on the PET membrane. The 2D image of the nanolithography result appears in Fig. 4, in which the holes and the piled-up area are easily distinguished from the other surface characteristics. Analysis of the created pits in terms of their dimensions, gives their real and precise geometrical characteristics, which are presented in Figs. 5 and 6.

It is interesting to notice that the shape of all four pits was almost the same, no matter how high the F_a values were, and approximately symmetrical, a fact that gives the evidence of vertical penetration. All the pits are accompanied by two pile-up regions, which surround the pits. The height and the width of the piled-up area were found to increase as the F_a increased from 254 to 760 nN (Fig. 5). Further increase of the F_a resulted only to the broadening and deepening of the pits (Fig. 5).

A clearer view of how the F_a affects the geometrical characteristics of the pits is given by the “aspect ratio”, i.e. the ratio of the width over the depth (Fig. 6). This parameter was found to significantly decrease from 12.7 to 8.9 as the F_a increases from 254 nN to 760 nN. From a phenomenological point of view, this behavior correlates the decrease of the pits’ width expansion rate and the simultaneous formation and growth of the piled-up area, as F_a increases.

4. Conclusions

The AFM in Contact mode operation was successfully used for nanolithography of soft materials, with H varying from 0.4 to 4 GPa. Well-shaped patterns were formed by a Si tip, instead of a diamond indenter tip that is mostly used for Nanoindentation. The results concerning the materials H and the calculated

P_a exerted by the AFM tip coming from Nanoindentation and SPM lithography, respectively, were contradicted. The applied forces by the SPM tip on the sample were typically in the range of 250 to 2520 nN. The exerted pressure on the samples was found to be at least equal or greater than their H in all cases, which satisfies the condition for permanent/plastic deformation by the SPM tip. Concerning the morphology of the patterns, the minimum size of indent/pit on PET was achieved and defined as 4 nm in depth. In addition, the F_a was correlated with the geometrical characteristics of the pit and it was found that for $F_a < 760$ nN, the applied force resulted to the increase of the materials piled-up volume and to the decrease of the aspect ratio of the created pits.

Acknowledgements

This work has been partially supported by the Hellenic Ministry of National Education and Religion Affairs under PYTHAGORAS II-ED 150 project.

References

- [1] G. Binnig, C. Gerbert, C. Quate, Phys. Rev. Lett. 56 (1986) 930.
- [2] G. Binnig, H. Rohrer, Sci. Am. 253 (2) (1985) 40.
- [3] U.F. Keyser, H.W. Schumacher, U. Zeltler, R.J. Haug, K. Eberl, Appl. Phys. Lett. 8 (1999) 1107.
- [4] M. Wendel, B. Irmer, J. Cortes, R. Kaiser, H. Lorentz, J.P. Kotthaus, A. Lorke, Superlattices Microstruct. 20 (1996) 350.
- [5] M. Wendel, S. Kühn, H. Lorenz, J.P. Kotthaus, M. Holland, Appl. Phys. Lett. 65 (1994) 1775.
- [6] M. Heyde, K. Rademann, B. Cappella, M. Geuss, H. Sturm, T. Spangenberg, H. Niehus, Rev. Sci. Instrum. 72 (2001) 136.
- [7] B. Cappella, H. Sturm, S.M. Weidner, Polymer 43 (2002) 4461.
- [8] N. Gadegaard, G. Marshall, C.D.W. Wilkinson, A.S.G. Curtis, Eur. Cells Mater. 7 (2004).
- [9] S. Logothetidis, M. Gioti, S. Lousinian, S. Fotiadou, Thin Solid Films 482 (2005) 126.
- [10] B. Cappella, H. Sturm, J. Appl. Phys. 91 (2002) 506.
- [11] W.C. Oliver, G.M. Pharr, J. Mater. Res. 7 (1992) 1564.
- [12] S.N. Kassavetis, S. Logothetidis, G.M. Matenoglou, Surf. Coat. Technol. 200 (2006) 6400.
- [13] C. Charitidis, M. Gioti, S. Logothetidis, Macromol. Symp. 205 (2004) 239.
- [14] U. Rabe, K. Janser, W. Arnold, Rev. Sci. Instrum. 67 (1996) 3281.
- [15] B. Bhushan, Handbook of Nanotechnology, Springer, Germany, 2004, p. 339.